

## Title page

## Limited co-localization of microbleeds and microstructural changes after severe traumatic brain injury

Running title: *Do microbleeds reflect traumatic axonal injury?*

Sara H. Andreassen<sup>1,2,3</sup>, Kasper W. Andersen<sup>1</sup>, Virginia Conde<sup>1,4</sup>, Tim B. Dyrby<sup>1,5</sup>, Oula Puonti<sup>1,5</sup>, Lars Peter Kammergaard<sup>2,6</sup>, Camilla G. Madsen<sup>1</sup>, Kristoffer H. Madsen<sup>1,5</sup>, Ingrid Poulsen<sup>2,7\*</sup>, Hartwig R. Siebner<sup>1,3,8\*</sup>

<sup>1</sup> Danish Research Centre for Magnetic Resonance (DRCMR), Centre for Functional and Diagnostic Imaging Research, Copenhagen University Hospital Hvidovre, Kettegaard Alle 30, 2650, Hvidovre, Denmark

<sup>2</sup> Research Unit on Brain Injury Rehabilitation Copenhagen (RUBRIC), Department of Neurorehabilitation, Traumatic Brain Injury, Copenhagen University Hospital Rigshospitalet, Copenhagen, Denmark

<sup>3</sup> Institute of Clinical Medicine, Faculty of Health and Medical Sciences, University of Copenhagen, Copenhagen, Denmark

<sup>4</sup> Clinical Neuroscience Laboratory, Institute of Psychology, Norwegian University of Science and Technology, Trondheim, Norway

<sup>5</sup> Department of Applied Mathematics and Computer Science, Technical University of Denmark, Kgs. Lyngby, Denmark

<sup>6</sup> Department of Neurology, Copenhagen University Hospital Rigshospitalet, Copenhagen, Denmark

<sup>7</sup> Department of Nursing Science, Faculty of Health, Aarhus University, Aarhus, Denmark

<sup>8</sup> Department for Neurology, Copenhagen University Hospital Bispebjerg, Copenhagen, Denmark

\* Contributed equally as senior authors

**Full author information:**

Sara Hesby Andreasen, MD

Tel: +4528122918, e-mail: sara.hesby.andreasen.03@regionh.dk

Address: Danish Research Centre for Magnetic Resonance (DRCMR), Centre for Functional and Diagnostic Imaging Research, Copenhagen University Hospital Hvidovre, Kettegaard Alle 30, 2650, Hvidovre, Denmark

Kasper Winter Andersen, Ph.D., Postdoc.

Tel: +4538622852, e-mail: kasperwj@drcmr.dk

Address: Danish Research Centre for Magnetic Resonance (DRCMR), Centre for Functional and Diagnostic Imaging Research, Copenhagen University Hospital Hvidovre, Kettegaard Alle 30, 2650, Hvidovre, Denmark

Virginia Conde, Ph.D.

Tel: +4542940615, e-mail: virginia.conde.ruiz@ntnu.no

Address: NTNU Dragvoll, Bygg 12, 12351A Trondheim, Norway

Tim Bjørn Dyrby, Associate Professor

Tel: +4538626542, e-mail: [timd@drcmr.dk](mailto:timd@drcmr.dk)

Address: Danish Research Centre for Magnetic Resonance (DRCMR), Centre for Functional and Diagnostic Imaging Research, Copenhagen University Hospital Hvidovre, Kettegaard Alle 30, 2650, Hvidovre, Denmark

Oula Puonti, PhD., Postdoc

Tel: +4538621184, e-mail: [oula.tapio.puonti@regionh.dk](mailto:oula.tapio.puonti@regionh.dk)

Address: Danish Research Centre for Magnetic Resonance (DRCMR), Centre for Functional and Diagnostic Imaging Research, Copenhagen University Hospital Hvidovre, Kettegaard Alle 30, 2650, Hvidovre, Denmark

Lars Peter Kammersgaard, DMSc, Consultant

Tel: +45 24244316, e-mail: [lars.peter.kammersgaard@regionh.dk](mailto:lars.peter.kammersgaard@regionh.dk)

Address: Research Unit on Brain Injury Rehabilitation Copenhagen (RUBRIC), Department of Neurorehabilitation, Traumatic Brain Injury, Copenhagen University Hospital Rigshospitalet, Kettegaard Allé 30, 2650 Hvidovre, Denmark

Camilla Gøbel Madsen, Ph.D., Consultant

Tel: +45 38620147, e-mail: [Camilla.Goebel.madsen@regionh.dk](mailto:Camilla.Goebel.madsen@regionh.dk)

Address: Danish Research Centre for Magnetic Resonance (DRCMR), Centre for Functional and Diagnostic Imaging Research, Copenhagen University Hospital Hvidovre, Kettegaard Alle 30, 2650, Hvidovre, Denmark

Kristoffer Hougaard Madsen, Associate Professor, Senior Researcher

Tel: +45 38622975 e-mail: [kristoffer.hougaard.madsen@regionh.dk](mailto:kristoffer.hougaard.madsen@regionh.dk)

Address: Danish Research Centre for Magnetic Resonance (DRCMR), Centre for Functional and Diagnostic Imaging Research, Copenhagen University Hospital Hvidovre, Kettegaard Alle 30, 2650, Hvidovre, Denmark

Ingrid Poulsen, Associate Professor, Research Director

Tel: +45 41277383, e-mail: [Ingrid.poulsen@regionh.dk](mailto:Ingrid.poulsen@regionh.dk)

Address: Research Unit on Brain Injury Rehabilitation Copenhagen (RUBRIC), Department of Neurorehabilitation, Traumatic Brain Injury, Copenhagen University Hospital Rigshospitalet, located at: Kettegaard Allé 30, 2650 Hvidovre, Denmark

Hartwig Roman Siebner, Professor, Research Director

Tel: +45 38626541, e-mail: [hartwig.roman.siebner@regionh.dk](mailto:hartwig.roman.siebner@regionh.dk)

Address: Danish Research Centre for Magnetic Resonance (DRCMR), Centre for Functional and Diagnostic Imaging Research, Copenhagen University Hospital Hvidovre, Kettegaard Alle 30, 2650, Hvidovre, Denmark

### **Corresponding authors:**

Hartwig Roman Siebner

Danish Research Centre for Magnetic Resonance (DRCMR), Centre for Functional and Diagnostic Imaging and Research, Copenhagen University Hospital Hvidovre, Kettegaard Allé 30, 2650 Hvidovre, Denmark.

E-mail: [Hartwig.roman.siebner@regionh.dk](mailto:Hartwig.roman.siebner@regionh.dk)

Ingrid Poulsen

Research Unit on Brain Injury Rehabilitation Copenhagen (RUBRIC), Department of Neurorehabilitation, Traumatic Brain Injury, Copenhagen University Hospital Rigshospitalet, located at: Kettegaard Allé 30, 2650 Hvidovre, Denmark

E-mail: [Ingrid.Poulsen@regionh.dk](mailto:Ingrid.Poulsen@regionh.dk)

## Abstract

Severe traumatic brain injury (TBI) produces shearing forces on long-range axons and brain vessels, causing axonal and vascular injury. To examine whether microbleeds and axonal injury co-localize after TBI, we performed whole-brain susceptibility-weighted imaging (SWI) and diffusion tensor imaging (DTI) in 14 patients during the subacute phase after severe TBI. SWI was used to determine the number and volumes of microbleeds in five brain regions: the fronto-temporal lobe, parieto-occipital lobe, mid-sagittal region (cingular cortex, parasagittal white matter and corpus callosum), deep nuclei (basal ganglia and thalamus), and brainstem. Averaged fractional anisotropy (FA) and mean diffusivity (MD) were measured to assess microstructural changes in the normal appearing white matter due to axonal injury in the same five regions. Regional expressions of microbleeds and microstructure was used in a partial least squares model to predict the impairment of consciousness in the subacute stage after TBI as measured with the Coma Recovery Scale-Revised (CRS-R). Only in the midsagittal region, expression of microbleeds correlated with regional changes in microstructure as revealed by DTI. Microbleeds and microstructural DTI-based metrics of deep but not superficial brain regions were able to predict individual CRS-R. Our results suggest that microbleeds are not strictly related to axonal pathology in other than the midsagittal region. While each measure alone was predictive, the combination of both metrics scaled best with individual CRS-R. Structural alterations in deep brain structures are relevant in terms of determining the severity of impaired consciousness in the acute stage after TBI.

**Keywords:** Traumatic brain injury; susceptibility weighted imaging; diffusion tensor imaging; microbleeds; traumatic axonal injury

## Introduction

Traumatic brain injury remains the leading cause of mortality and long-term disability in young individuals in the western world.<sup>1</sup> Clinical assessment of traumatic brain injury (TBI) severity is challenging. After the acute comatose state, patients surviving severe TBI will often go through distinct phases in their awakening process, namely the unresponsive wakefulness syndrome (UWS) with preserved arousal but no signs of consciousness and the minimally conscious state (MCS) with preserved arousal and reproducible but fluctuating behavioral signs of consciousness.<sup>2, 3</sup> The spectrum of pathological lowered consciousness ranging from coma to MCS are known as disorders of consciousness (DOC).<sup>4</sup>

The duration of DOC is the only well-established clinical marker that indicates the severity of TBI.<sup>5,6</sup> Since DOC can only be defined retrospectively when the patient has regained consciousness, DOC cannot be used as prognostic marker in TBI patients with DOC. Tensile stress induced traumatic axonal injury (TAI) is considered the major cause of prolonged neurological deficits and impaired consciousness following severe TBI. The strain comes from high velocity translational and rotational forces of the brain and results in disconnection of long-range circuitry.<sup>7</sup> Post-traumatic lowered level of consciousness is believed an emergent property of the reduced cortico-cortical and thalamo-cortical connectivity from these traumatic axonal injuries, and therefore biomarkers of axonal integrity are regarded the answer to evaluation of TBI severity.<sup>8,9</sup>

TAI is microscopic in nature and largely evades conventional imaging.<sup>10</sup> The associated hemosiderin deposits from microbleeds on the other hand give rise to signal voids in hemorrhage sensitive imaging, such as T2\*-gradient recalled-echo (GRE) and susceptibility weighted imaging (SWI).<sup>11</sup> Both can easily be assessed in the majority of clinical facilities. Traumatic microbleeds have therefore been used to infer the degree of tensile stress inflicted in the brain tissue and as a proxy marker of TAI. However, there exists no structural investigations that systematically assess how much traumatic microbleeds and axonal injury co-localize in the human brain. Given the solid histological evidence of more than 400 severe TBI cases linking TAI to clinical severity and oppositely very mixed results from studies linking traumatic microbleeds in MRI to clinical severity, we felt motivated to examine the topographical coherence between traumatic axonal and vascular injury.<sup>12-18</sup>

Diffusion tensor imaging (DTI) can be used to probe the microstructure of the brain and is sensitive to changes in the white matter (WM). DTI is currently valued the best in-vivo estimation of TAI in TBI research.<sup>19</sup> Combining DTI and hemorrhage sensitive imaging, offers a unique test of the association between axonal integrity and vascular lesions, and provides access to investigate the magnitude and spatial coherence of the two types of injury. Four small studies in mild to moderate TBI have already included the two modalities, but only less than half of the included patients had any microbleeds, and so the conclusions are sparse.<sup>17, 20-22</sup> One study of moderate to severe TBI has addressed the effect on longitudinal DTI from traumatic microbleeds in the acute phase and therefore extracted DTI metrics in regions of interest (ROIs) selected by the presence of microbleeds.<sup>23</sup> Only a single recent retrospective study looked at DTI metrics in normal appearing white matter (NAWM) of mixed severity TBI patients and found that traumatic microbleeds in basal ganglia and thalamus correlated to fractional anisotropy (FA) in subcortical NAWM. No regions showed significant co-localization between microbleeds and DTI parameters.<sup>24</sup>

To our knowledge, no study has systematically investigated whether traumatic microbleeds co-localize with TAI of NAWM, as indexed by DTI, in the subacute stage of severe TBI and has related these measures to clinical severity. Inspired by the inconclusive results of studies linking traumatic microbleeds to prognosis,<sup>12-18</sup> we hypothesized that vascular and neural structures might display different sensitivity to shearing injury in different brain territories. We therefore expected that the regional post-traumatic expression of microbleeds as revealed by SWI lesions and regional alterations in white-matter microstructure (as captured by FA and mean diffusivity (MD)) would show a discrepancy in their spatial expression at the subacute stage after severe TBI. Furthermore, we expected that the regional load of traumatic microbleeds can be used to predict the individual level of impaired consciousness in the subacute stage of TBI, when scans and clinical tests are performed at the same time points.

## Materials and Methods

This study is part of a larger prospective neuroimaging project on severe TBI, for a full review please refer to reference<sup>25</sup>

### Patients

We recruited patients in the subacute phase after severe TBI, when they were admitted to a highly specialized department for neurorehabilitation at a Danish university hospital from October 2014 to February 2018. Inclusion criteria were closed-head TBI in the states of unresponsive wakefulness syndrome (UWS), minimal conscious state (MCS) or the state of confusion. Exclusion criteria were contraindications for MRI, patients who had undergone craniectomies, large intracerebral hemorrhages or infarctions, structural lesions in the brain stem and / or patients with TBI and locked-in syndrome due to motor pathway lesions. Seventeen patients were included after receiving informed consent from patients' close relative and general practitioner. However, two patients could not cooperate in the scanning sessions and one patient only had a single scan with severe artefacts, resulting in inclusion of 14 patients. Twenty-seven healthy controls were included, where six subsequently were excluded due to unexpected findings in the initial MRI session or dropout of the second session (Table 1). In the inclusion period, totally 143 patients with severe TBI were admitted to the rehabilitation department but could not be included due to the inclusion and exclusion criteria or that relatives did not want the patient to participate. All patients were extremely severely injured, defined by both initial Glasgow Coma Scale score of median three and Injury Severity Scale score of median 31 (the score range with increasing severity from 0 to 75, where 75 is regarded unsurvivable), and a Rotterdam CT cerebrum score at time of injury of median 2 (score range with increasing severity from 1-6).<sup>26, 27</sup> Duration of post traumatic amnesia (PTA) is the clinical variable closest associated with the severity of the brain injury.<sup>6</sup> In our cohort the average PTA was 207 days (above 70 days are considered extremely severe brain injury).<sup>28</sup> The mean number of days from TBI until the project MRI was 44. Patients' condition and demand of intensive therapy varied and the average time from trauma to the MRI scan varied accordingly within a range of 26 to 81 days (Table 1). One patient had received



anticoagulant medication prior to injury and all patients either received antiplatelet or anticoagulant medication as preventive anti-thrombotic treatment after injury (n=14). Four patients were prone to non-traumatic microbleeds prior to injury because of arterial hypertension (n=3) or atrial fibrillation (n=1).

Ethical approval was obtained by the local ethics committee of the Capital region of Denmark (no H-4-2013-186) and by the Danish Data Protection Authority (no 2007-58-0015). The project followed the Declaration of Helsinki; ethical principles for medical research involving human subjects. Informed consent was obtained from patient's proxy and general practitioner. Patients themselves were asked for informed consent as soon as they were capable to reliably perceive and understand information.

[TABLE 1 here]

### **Clinical level of consciousness**

The coma recovery scale revised (CRS-R) was used as the clinical measure to assess recovery from coma. CRS-R is a bedside behavior-based assessment of five cognitive domains: auditory and visual perception, motor, verbal and communicative performance, and one observational assessment of level of arousal.<sup>29</sup> The CRS-R has proven to be superior to unstructured clinical evaluation performed by experts, raising the detection-rate of consciousness by 40% and is considered the golden standard of clinical test for consciousness.<sup>30</sup> CRS-R detects the lowest levels of disorders of consciousness (DOC), separating the unresponsive wakeful syndrome/vegetative state from the minimal conscious state. This segregation is crucial to both the overall prognosis of emerging to full consciousness and to commence of neuro-rehabilitation, which again assures the best possible functional outcome.<sup>31, 32</sup> Patients were assessed weekly from inclusion until discharge from the TBI department.

### **MRI acquisition**

Imaging was acquired on a 3 tesla MRI scanner (Siemens Verio, Siemens Medical Systems, Germany) using a 32-channel head coil. The image protocol consisted of the following sequences acquired in 1 mm<sup>3</sup> isotropic resolution: 3D T1-weighted (T1w) Magnetization

Prepared Rapid Gradient Echo (MPRAGE), (repetition time (TR) = 1900 ms; echo time (TE) = 2.23 ms; Field of View (FoV) of 250×250 mm; slab thickness 176 mm), 3D T2-weighted (T2w) SPACE (TR = 3200 ms; TE = 409 ms; FoV = 250×250 mm; slab thickness 176 mm), 3D Fluid Attenuation Inversion Recovery (FLAIR) (TR = 5000 ms; TE = 395 ms; FoV = 250×250 mm; slab thickness 160mm). Susceptibility Weighted Imaging (SWI) (TR = 28 ms; TE = 20.0 ms; FoV=230mm×173mm) was acquired in resolution of 0.8×0.7×1.2 mm<sup>3</sup> and diffusion weighted imaging with 10 b=0 s/mm<sup>2</sup> and b=1000 s/mm<sup>2</sup> in 61 directions (TR = 11060 ms; TE = 78 ms) was acquired in 2.3 mm<sup>3</sup> isotropic resolution. There were no major scanning upgrades during the project. No anesthetics were used, only patients' prescription medication, occasionally including tranquilizers.

The MRI scans included in this study were acquired as part of a larger neuroimaging project at two time points during the sub-acute in-hospital rehabilitation period, while patients were treated at the department of Neurorehabilitation, TBI Unit.<sup>25</sup> Whenever MRI scans had good quality, we included the first MRI scan: In 12 of the 14 patients, DWI measures were derived from the initial diffusion-weighted MRI scan taken in the first week of in-hospital rehabilitation. In the remaining two patients, DWI measures had to be calculated from the second diffusion-weighted MRI scan taken in week 4 of in-hospital rehabilitation because of insufficient image quality of the first DWI scan due to excessive head movements. The variables "Time from injury to scan" and the variable "coma recovery scale revised (CRS-R)<sup>29</sup> score at the time of scan", presented in Table 1 are referring to the scanning session used for DWI measures. Healthy controls were included and scanned consecutively to match patient population.

### DTI processing

DWI data were preprocessed using an in-house pipeline applying Gibbs unringing<sup>33</sup> and susceptibility, motion, and eddy current correction using FSL's *topup* and *eddy* (<https://fsl.fmrib.ox.ac.uk/fsl/fslwiki/>).<sup>34, 35</sup> FA and MD maps were calculated using FSL's *dtifit*.

### Traumatic microbleed and FLAIR hyperintensity drawing

Traumatic microbleeds were manually outlined on the SWI images using JIM (Xinapse Systems, Leicester, UK, [www.xinapse.com](http://www.xinapse.com)). JIM allows simultaneous reviewing of the lesion on FLAIR, T1w, T2w and the SWI phase images, to minimize inclusion of traumatic microbleeds mimics (veins, calcifications etc.). Traumatic microbleeds were defined as hemorrhages caused by strain on the vascular system; thus surface-near cortical bleeds likely to be excoriations against the inner skull table and likewise small bleeds in intimacy of mass lesions were not included in the traumatic microbleeds outline.<sup>36</sup> No formal size criteria exists for traumatic microbleeds,<sup>37</sup> only for cerebral microbleeds of other origins.<sup>38</sup> Traumatic microbleeds are not always solitary punctuate bleeds, they can occasionally be large, if arising from a deep GM arterial tear or by several minor bleeds aggregating into clusters.<sup>39</sup> We outlined small bleeds (single bleeds of minimum 2 voxels and less than 5 mm in diameter or aggregated clusters of minor bleeds) in the white matter (WM) or at WM-grey matter (GM) junctions.

We defined FLAIR white matter hyperintensities (WMH) as minimum 2 voxels on minimum 2 consecutive slices, of clearly higher signal intensity relative to the surrounding tissue and not intimately related to focal lesions. FLAIR WMH are commonly used as a correlate of the TAI without accompanying microbleeds, often referred as non-hemorrhagic TAI. WMH are also closely related to age, small vessel disease in patients with hypertension, diabetes or hypercholesterolemia and lifestyle risk factors e.g. smoking, heart disease, dementia and some psychiatric disorders and demyelination diseases e.g. multiple sclerosis.<sup>40, 41</sup> Though many TBI studies have shown close association of WMH to outcome,<sup>13, 14, 18, 42</sup> FLAIR hyperintensities inherently have low specificity for TAI.

In seven of the 14 patients, the initial SWI and FLAIR scans, acquired in the first week of subacute in-hospital rehabilitation, were of insufficient quality due to motion artifacts. Therefore, the outline of microbleeds was performed on the second SWI scan that were acquired in the fifth week of in-hospital rehabilitation. The number or volume of microbleeds should not change within a few weeks as the susceptibility-related hypo-intensities is expected to be stable over time. Hereafter the outlines of the traumatic

microbleeds and FLAIR hyperintensities were co-registered to the T1w image from the same session, which we use the DWI. This maneuver ensured that all traumatic microbleeds, FLAIR hyperintensities and DWI measures were obtained at the earliest time point possible after injury, and within as tight a time window as possible justifying comparison between subjects. All outlines were performed by author SHA and supervised by neuro-radiologist author CM. Potential microbleeds and FLAIR hyperintensities were not outlined in the healthy controls (Figure 1).

[FIGURE 1 here]

[FIGURE 2 here]

### Brain segmentation

To enable a coarse assessment of spatial distribution, we segmented the brain into five regions, which is sensitive to anterior-posterior as well as cortical vs. deep gradients, using the following procedure. Each subject's T1w image were co-registered with the SWI using SPM 12 (rev. 6470) and run through Freesurfer version 6.0 *recon-all* pipeline to produce volume segmentations of the neuroanatomical structures and a surface parcellation of the cortex. The resulting segmentations were individually reviewed, corrected and reprocessed. Based on the Freesurfer segmentation we grouped the brain into five regions: (1) fronto-temporal region; (2) parieto-occipital region; (3) midsagittal region (corpus callosum, cingulate and parasagittal WM); (4) brainstem (pons, midbrain and medulla); and (5) basal ganglia (caudate, putamen, pallidum) and thalamus. Non-assigned voxels in cerebral white matter were assigned to one of the five regions based on shortest distance to cortical label. Of note, Freesurfer WM parcellation of corpus callosum is the 3-voxel wide callosal junction between the 2 hemispheres. The WM lobe parcellation is based on cortical parcellation, so the parasagittal WM and GM are more precisely defined the cingular and subcingular WM. The midsagittal region thereby includes most mesial brain in both the sagittal and coronal plane.

We grouped the lesions into connected clusters based on a neighborhood of the six closest voxels using Matlab R2017A (The MathWorks, Inc., Natick, Massachusetts, United States). Then the number and volume of lesions belonging to each of the five brain regions were

calculated. When the lesion clusters overlapped with more than one of the brain segmentations, we assigned the lesions to the region containing most of the volume and recorded this as one count of lesion incidence in the region. We also recorded the volume overlap, in voxels, between the brain regions and the lesion mask.

### Data extraction

The T1w image was co-registered to the DTI space using FSL's *flirt* and the same spatial transformation was applied to the brain segmentations. *Flirt* is a linear registration tool, which was used to co-register the T1-weighted image to the FA map using six degrees of freedom using the correlation ratio as cost-function. A lesion mask of all FLAIR hyperintensities, traumatic microbleeds and focal lesions (including parenchyma damage secondary to surgical procedures such as ventricular drainage) were made. Voxels from this mask were removed from the brain segmentation before further analyzes (Figure 1). This step ensured that the DTI measures reflected the diffuse axonal injury and not focal or vascular injury. Each of the five brain regions were eroded by a single voxel in all dimensions. For four of the five brain regions (i.e. the three hemispheric regions and brainstem), we only considered voxels with  $FA > 0.3$  for analyses of regional FA and MD. These procedures reduce WM-GM and WM-CSF partial volume effects and leave only WM voxels with coherent fiber architecture for analysis.<sup>43</sup> For the basal ganglia-thalamus region, no FA threshold was applied for voxel selection, because these deep brain nuclei consist only of GM. We extracted the average FA and MD values within the five brain regions. For analyses within the TBI group, we age-adjusted FA and MD according to a linear trend found in the HC group within each of the five ROIs.

### Statistical analyses

All statistical analyses were performed in Matlab R2017A (The MathWorks, Inc., Natick, Massachusetts, United States). Group comparison (patients versus healthy matched controls) within each of the five brain regions of FA and MD were calculated using 2-sample t-tests as proof of concept that DTI measures are elaborate measures of TAI. FA and MD were correlated to traumatic microbleed counts and volumes in the same regions using Spearman's rank correlation controlling for age. We set the significance level to

$p < 0.05$  (uncorrected) and use Bonferroni correction for multiple comparisons in the five brain regions, corresponding to an uncorrected significance level of  $p < 0.01$ .

The diagnostic potential of the two modalities (DTI and microbleeds) was post hoc explored to predict the patients' consciousness state (CRS-R score) by means of data collected at the same timepoints. This was done using partial least squares regression (PLS) using Matlab's *plsregress* function with the number of components  $n=1$ . We used a leave-one-out cross-validation (LOOCV) scheme, which iteratively trains a model by leaving a sample (here patient) out of the model estimation and then predicts the CRS-R score of the left-out-sample. We would like to emphasize that in the present paper, we did not use the PLS LOOCV approach for prognostication of outcome, but as a means of predicting the patient's clinical state at the time of imaging, namely in the subacute stage after severe TBI. The resulting correlation coefficient between the true and predicted CRS-R indicates how well the model and selected variables can be used to predict unseen data. According to the centripetal model, the central and deep lesions are associated to worse outcome than the more superficial lesions.<sup>13, 14, 17, 44-46</sup> We therefore made models separately for the hemispheric structures (fronto-temporal and parieto-occipital) and deep structures (midsagittal region, brainstem, and basal ganglia-thalamus). In addition, we ran the analyses separately for each of the five brain regions. For each of the mentioned groupings of regions, we tested these three variable groupings:

- 1) Uni-modal model using traumatic microbleed counts and volumes as variables.
- 2) Uni-modal model using DTI variables (FA and MD) as variables.
- 3) Bi-modal model combining FA, MD and traumatic microbleed counts and volumes as variables.

To calculate unbiased  $p$ -values for the prediction model, we used permutation tests to build an empirical null-distribution. This null-distribution was calculated with 10,000 LOOCV evaluations, where the CRS-R value was permuted across patients.

## Results

### Group differences in diffusion tensor imaging metrics

Compared with HC, TBI patients had significantly ( $p < 0.01$ ) lower FA in all regions except for the basal ganglia-thalamic region, in which there were a trend towards that FA was higher in patients ( $p = 0.02$ ) (Figure 3, bottom-left). In addition, TBI patients had significantly higher MD in basal ganglia-thalamic, parieto-occipital, and fronto-temporal (all  $p < 0.001$ ). There was a trend towards higher MD in the mid-sagittal region ( $p = 0.02$ ), but no group difference in the brainstem (Figure 3, bottom-right).

[FIGURE 3 here]

### Traumatic microbleeds and FLAIR hyperintensities

The patients had few or moderate FLAIR hyperintensities. The median number of WMH was 3 (range 0-32) for the fronto-temporal region, 2 (range 0-16) for the parieto-occipital region, 0 (range 0-3) for the mid-sagittal region, 0 (range 0-1) for brainstem and 0 (range 0-2) for the basal ganglia-thalamus region. Since relatively few WMH was present, and most of them was in the hemispheric regions, we did not consider them further.

Count and volume of traumatic microbleeds are shown in Table 2 and in Figure 3 (top). The fronto-temporal region had the highest count (median  $n = 56$ ) and volume (mean  $3095 \text{mm}^3$ ) of microbleeds. The number of microbleeds were more evenly distributed in the other brain regions with medians 14 in the parieto-occipital, 12 in the mid-sagittal and basal ganglia-thalamus regions and 3 in the brainstem.

Only the midsagittal region showed significant negative relationship between FA and number ( $r = -0.71$ ,  $p = 0.004$ ) and volume ( $r = -0.68$ ,  $p = 0.008$ ) of traumatic microbleeds (Figure 4), suggesting that higher lesion count and volume is associated with less FA in the midsagittal region. No other regions showed significant correlations with either FA or MD (all  $p > 0.05$ ).

[TABLE 2 here]

[FIGURE 4 here]

To explore the possibility whether the regional axonal injury in one region is associated with microvascular damage in other brain regions, we performed additional exploratory correlational analyses (Spearman's rank correlations). Mean FA in the mid-sagittal region (CC and CING) showed a negative relationship - not only with the TMB number and volume in the same area - but also with the number of TMB in other subcortical mid-sagittal regions, namely the thalamus/basal ganglia and brainstem regions. Mid-sagittal hemispheric FA values also scaled negatively with the volume of TMB in thalamus/basal ganglia and posterior hemispheric white matter (PAR/OCC). These findings can only be considered as trends as they would not survive correction for multiple comparisons, given that the non-corrected p-values ranged between 0.043 and 0.023. No trend correlations were found between mean regional MD values and regional number or lesion of TMB.

### **Predicting conscious level as reflected by CRS-R score in subacute TBI stage**

Regional expression of microbleeds as well as microstructure in the deep structures (midsagittal, brainstem and basal ganglia-thalamus) were able to significantly predict the level of consciousness expressed by the CRS-R scores (count and volume of microbleeds:  $r=0.65$ ,  $p=0.01$ ; FA, and MD:  $r=0.59$ ,  $p=0.02$ ; count and volume of microbleeds, FA, and MD:  $r=0.72$ ,  $p=0.003$ ) (Figure 5). However, using the DTI and microbleeds information extracted from the hemispheric regions (fronto-temporal and parieto-occipital), were not able to significantly predict the CRS-R scores (all  $p>0.05$ ).

Using the same analysis approach in the individual five brain regions returned a more detailed perspective of which modality has more weight in the different regions. Both the bimodal model of the midsagittal, basal ganglia and thalamus and the brainstem regions were able to significantly predict the CRS-R score ( $p<0.01$ ) (Figure 6).

[FIGURE 5 here]

[FIGURE 6 here]

### **Discussion**

We found that the regional expression of traumatic microbleeds only co-localizes with regional microstructural changes as captured with DTI in the mid-sagittal portion of the cerebral hemisphere. Only in this region, the number and volume of microbleeds scaled



positively and linearly with regional FA. The remaining four regions showed no consistent correlations between regional microbleed load and regional microstructure. Critically, only brain tissue not affected by microbleeds was considered for assessing regional FA to ensure that DTI metrics were not directly influenced by the microbleeds themselves. These findings show that with the exception of the mid-sagittal region, traumatic vascular and axonal injury are not coherently expressed in the human brain. Thus, MRI-metrics of microbleeds and microstructure cannot be interchangeably used in the neuro-radiological assessment of TBI. In particular, the regional expression of microbleeds which can be easily quantified by MRI cannot be used as a proxy of regional axonal injury. The available post mortem data on the spatial expression of traumatic microbleeds is in agreement with our findings.<sup>36</sup> Adams reports that microbleeds often accompanied TAI lesions in corpus callosum, whereas microbleeds in other brain territories are caused by various etiologies, such as of local contusion or distortion of the bloodvessels.<sup>36</sup> We argue that microbleeds and TAI are two complementary indicators of the severity of shear strain injury with different brain regions displaying different susceptibility to vascular or axonal damage.

The lack of correlation between microbleeds and mean regional FA in four out of five brain regions might, at least partially, be explained by using DTI as imaging modality to assess cerebral microstructural damage. We used two DTI-based metrics for assessing cerebral microstructure, FA and MD. While FA reflects the degree of directionality in a given voxel, MD indicates the magnitude of diffusion in the voxel independently of the diffusion direction. FA values were very high in the med-sagittal region containing the corpus callosum and this region showed the strongest degree in FA in the TBI group relative to healthy controls. This is not surprising as the axons share highly similar directions in the corpus callosum and damage of this region will decrease FA. Other brain regions display lower mean FA values because of a less regular orientation of white matter fibers and because they contain relatively more grey matter structures. Therefore, the fact that we only found a correlation between regional microbleed expression and mean FA (as index of axonal damage) in the mid-sagittal brain region may be due to the fact that our DTI-marker was particularly suited to probe TAI in this region but less reliable in the other regions. Microstructural metrics derived from diffusion-sensitive MRI acquisitions that go beyond

routine DWI acquisition methods might be better suited to capture TAI in those brain regions containing tissue microstructures that are heterogenous in size, shape and orientation.<sup>47, 48</sup>

How may microbleeds contribute to TBI-induced brain damage? Extravasated blood in the central nervous system activates cytotoxic, oxidative and inflammatory cascades. The inflammatory response cause local breakdown of the blood-brain barrier, leading to edema and subsequent brain swelling which may lead to wide spread ischemia.<sup>49, 50</sup> These mechanisms driven by traumatic vascular injury could contribute to TBI-induced brain pathology and clinical impairment of consciousness. We therefore explored whether our SWI-based assessment of microbleeds and the DTI-based estimates of regional microstructure obtained in the subacute stage of TBI would predict the severity of impaired consciousness as reflected by the individual CRS-R score. We pooled the mean SWI- and DTI-based metrics of the two hemispheric regions and the three deep brain regions to see whether we could derive the individual impairment of consciousness at the time of MRI examination from our regional MRI metrics. Only the MRI metrics of the deep brain structures but not the hemispheric structures scaled positively with impaired consciousness. Our LOOCV showed that both the traumatic microbleeds and the DTI-based metrics could predict the individual CRS-R score. The number and volume of microbleeds in the mid-sagittal region, brain stem, thalamus, and basal ganglia showed a linear positive relationship with individual CRS-R scores. The same was true when considering mean regional FA and MD of the brain stem, thalamus, and basal ganglia. When considering SWI- and DTI-based MRI metrics together, prediction of the individual impairment of consciousness improved further, pointing to the possibility that both MRI metrics provided complementary information about TBI-induced brain damage. Including both MRI modalities (SWI and DTI), a significant prediction of the individual CRS-R score was also possible based on the microbleeds and DTI-changes in a single deep region with comparable prediction performance. Taken together, the results indicate that the injury load in terms of microbleeds (SWI) and microstructural change (DTI) in the deep brain structures are complementary pathology markers of shear strain injury. Further, it might be sufficient to only assess microbleeds and estimate mean FA and MD in a single deep

brain region (e.g. mid-sagittal hemispheric region or brain stem or basal ganglia-thalamus) for an MRI-based prediction of the level of impaired consciousness in the subacute stage.

The finding that structural changes in mesial and deep brain structures (mid-sagittal, brainstem, basal ganglia and thalamus) predicted individual CRS-R but not the structural alterations in more superficial structures of the cerebral hemispheres (fronto-temporal and parieto-occipital regions) is in good agreement with the topographical distribution of shear strain injury caused by TBI.<sup>9, 36, 51</sup> According to the Ommaya-Gennarelli model, the magnitude of applied shear force during the trauma shows a centripetal gradient because the degree of shear-strain and deformation of brain tissue increases with the distance from the centre of mass.<sup>49</sup> Hence, central parts of the brain are better protected and will only be affected at higher force accelerations, decelerations and rotations<sup>52, 53</sup>. This implies that only a very strong trauma will cause sufficient shear forces to cause TAI and microbleeds in deeper brain structures. From a bio-mechanical point of view, one should therefore focus on tissue alterations of deep structures and not on superficial regions with highest traumatic microbleeds load. Accordingly, studies reporting an association between traumatic microbleeds and outcome ascribe unfavorable outcome to microbleeds in the medulla-midbrain territories<sup>44, 45, 54</sup> or basal ganglia -thalamic region.<sup>12, 54</sup> This notion is also plausible from a neurobiological perspective. The ascending reticular activating system (ARAS) responsible for arousal and wakefulness and networks of vegetative homeostasis are located in the upper brainstem and midbrain.<sup>55</sup> Likewise, thalamic-basal ganglia projecting to mesial forebrain have been implicated in the formation of awareness.<sup>56, 57</sup>

### Limitations

The main limitation of this study is the relatively small sample size of 14 patients. We expect that the benefit of concurrent assessment of traumatic microbleeds with SWI and microstructure with TBI would become more evident in a larger cohort. Nonetheless, the sample size was sufficient to identify distinct spatial patterns which are in good agreement with previous neuroanatomical and neuroimaging work. Another potential limitation is that age could influence the vascular susceptibility to shear strain injury. We have

corrected for age in our statistical analyses but were unable to address the influence of age which needs to be addressed in future studies. Interaction of traumatic microbleeds and age has already been studied by Toth 2018, who found no such effect.<sup>24</sup>

## Conclusion

Applying a regional analysis which considered five brain regions, we found that only in the mid-sagittal region, the regional traumatic microbleeds load reflected the microstructural change as revealed by DTI. Therefore, we conclude that SWI-based assessment of microbleeds and DTI-based assessment of microstructural changes in the subacute stage provide complementary insights into the structural sequelae of severe TBI. Hence, traumatic microbleeds should not be considered as a simple proxy for TAI. Our results further stress the relevance of post-traumatic alterations in deep brain structures as they indicate a more severe traumatic impact on the brain affecting key brain structures involved in vigilance and awareness. Further studies are warranted which assess the clinical value of combining an SWI-based assessment of traumatic microbleeds with DTI of microstructure in deep brain structures to predict the individual severity of DOC in the subacute stage after severe TBI.

## Acknowledgements

We thank patients and relatives for participation in the study. Furthermore, we thank Sussi Larsen (radiographer at DRMR), Tue H. Pedersen (postdoc, TBI Department), Karen B. Larsen and Mia M. Wolffbrandt (research nurse, TBI Department) and the staff at the TBI Department at Rigshospitalet for their support. The study was funded by the Capital Region of Denmark (Region H, grant number R135-A4841), the Lundbeck Foundation (grant number R126-2012-12422), and the Danish Council for Independent Research, Section of Medical Sciences (DFF-FSS, grant number DFF - 1331-00172). Hartwig R. Siebner holds a 5-year professorship in precision medicine at the Faculty of Health Sciences and Medicine, University of Copenhagen which is sponsored by the Lundbeck Foundation (Grant Nr. R186-2015-2138).

## Author Disclosure Statement

Hartwig R. Siebner has received honoraria as speaker from Sanofi Genzyme and as editor from Elsevier Publishers, Amsterdam, The Netherlands and Springer Publishing, Stuttgart, Germany and has received a research fund from Biogen Idec and Novartis.

## References

1. Dewan, M.C., Rattani, A., Gupta, S., Baticulon, R.E., Hung, Y.C., Punchak, M., Agrawal, A., Adeleye, A.O., Shrivastava, M.G., Rubiano, A.M., Rosenfeld, J.V. and Park, K.B. (2018). Estimating the global incidence of traumatic brain injury. *J Neurosurg*, 1-18.
2. Laureys, S., Celesia, G.G., Cohadon, F., Lavrijsen, J., Leon-Carrion, J., Sannita, W.G., Szabon, L., Schmutzhard, E., von Wild, K.R., Zeman, A., Dolce, G. and European Task Force on Disorders of, C. (2010). Unresponsive wakefulness syndrome: a new name for the vegetative state or apallic syndrome. *BMC Med* 8, 68.
3. Giacino, J.T., Ashwal, S., Childs, N., Cranford, R., Jennett, B., Katz, D.I., Kelly, J.P., Rosenberg, J.H., Whyte, J., Zafonte, R.D. and Zasler, N.D. (2002). The minimally conscious state: definition and diagnostic criteria. *Neurology* 58, 349-353.
4. Bernat, J.L. (2006). Chronic disorders of consciousness. *Lancet (London, England)* 367, 1181-1192.
5. Maas, A.I., Harrison-Felix, C.L., Menon, D., Adelson, P.D., Balkin, T., Bullock, R., Engel, D.C., Gordon, W., Langlois-Orman, J., Lew, H.L., Robertson, C., Temkin, N., Valadka, A., Verfaellie, M., Wainwright, M., Wright, D.W. and Schwab, K. (2011). Standardizing data collection in traumatic brain injury. *J Neurotrauma* 28, 177-187.
6. Ponsford, J.L., Spitz, G. and McKenzie, D. (2016). Using Post-Traumatic Amnesia To Predict Outcome after Traumatic Brain Injury. *J Neurotrauma* 33, 997-1004.
7. Gennarelli T.A, G. (1998). Neuropathology of the head injury. In: *Seminars in clinical neuropsychiatry*, pps. 160-175.
8. Meythaler, J.M., Peduzzi, J.D., Eleftheriou, E. and Novack, T.A. (2001). Current concepts: Diffuse axonal injury–associated traumatic brain injury. *Archives of Physical Medicine and Rehabilitation* 82, 1461-1471.
9. Gennarelli, T.A. and Graham, D.I. (1998). Neuropathology of the Head Injuries. *Seminars in clinical neuropsychiatry* 3, 160-175.

10. Toth, A., Kovacs, N., Tamas, V., Kornyei, B., Nagy, M., Horvath, A., Rostas, T., Bogner, P., Janszky, J., Doczi, T., Buki, A. and Schwarcz, A. (2016). Microbleeds may expand acutely after traumatic brain injury. *Neurosci Lett* 617, 207-212.
11. Haacke, E.M. (2011). Chapter1. Introduction to Susceptibility Weighted Imaging. In: *Susceptibility Weighted Imaging in MRI: Basic Concepts and Clinical Applications*. . Mark Haacke, J.R. (ed). Wiley-Blackwell.
12. Cicuendez, M., Castano-Leon, A., Ramos, A., Hilario, A., Gomez, P.A. and Lagares, A. (2018). The added prognostic value of MR imaging in Traumatic Brain Injury: the importance of TAI lesions when performing an ordinal logistic regression. *J Neuroradiol*.
13. Cody A. Chastain, U.E.O., Michelle Zipperman, Elliot Joo, Stephen Ashwal, Lori A. Shutter, and Karen A. Tong (2009). Predicting Outcomes of Traumatic Brain Injury by Imaging Modality and Injury Distribution. *J Neurotrauma* 26, 1183–1196.
14. Moen, K.G., Brezova, V., Skandsen, T., Haberg, A.K., Folvik, M. and Vik, A. (2014). Traumatic axonal injury: the prognostic value of lesion load in corpus callosum, brain stem, and thalamus in different magnetic resonance imaging sequences. *J Neurotrauma* 31, 1486-1496.
15. Moen, K.G., Skandsen, T., Folvik, M., Brezova, V., Kvistad, K.A., Rydland, J., Manley, G.T. and Vik, A. (2012). A longitudinal MRI study of traumatic axonal injury in patients with moderate and severe traumatic brain injury. *J Neurol Neurosurg Psychiatry* 83, 1193-1200.
16. Rainer Scheid, C.P., Oliver Gruber, Christopher Wiggins, and D. Yves von Cramon (2003). Diffuse Axonal Injury Associated with Chronic Traumatic Brain Injury- Evidence from T2\*-weighted Gradient-echo Imaging at 3 T. *AJNR Am J Neuroradiol* 24, 1049–1056.
17. Raj Kumar, M.H., Rakesh K. Gupta, Khader M. Hasan, Mohammad Haris, Atul K. Agarwal, C.M. Pandey, and Ponnada A. Narayana (2009). Serial Changes in the White Matter Diffusion Tensor Imaging Metrics in Moderate Traumatic Brain Injury and Correlation with Neuro-Cognitive Function. *J Neurotrauma*, 481-495.

18. Spitz, G., Maller, J.J., Ng, A., O'Sullivan, R., Ferris, N.J. and Ponsford, J.L. (2013). Detecting lesions after traumatic brain injury using susceptibility weighted imaging: a comparison with fluid-attenuated inversion recovery and correlation with clinical outcome. *J Neurotrauma* 30, 2038-2050.
19. Hulkower, M.B., Poliak, D.B., Rosenbaum, S.B., Zimmerman, M.E. and Lipton, M.L. (2013). A decade of DTI in traumatic brain injury: 10 years and 100 articles later. *AJNR Am J Neuroradiol* 34, 2064-2074.
20. Kou, R.B., R; Haacke, E. (2009). Susceptibility Weighted Imaging Complements Diffusion Tensor Imaging in Traumatic Brain Injury In: *International Society for Magnetic Resonance in Medicine. Proc Intl. Soc. Mag.Reson.Med.*
21. Asano Y, S.J., Okumura A, Aki T, Takenaka S, Miwa K, Yamada M, Ito T, Yokoyama K (2012). Utility of Fractional Anisotropy Imaging Analyzed by Statistical Parametric Mapping for Detecting Minute Brain Lesions in Chronic-Stage Patients Who Had Mild or Moderate Traumatic Brain Injury. *Neurol Med Chir*, 31-40.
22. Yukinori Akiyama, K.M., Kuniaki Harada, Yoshihiro Minamida, Tadashi Nonaka, Izumi Koyanagi, Yasufumi Asai, Kiyohiro Houkin (2009). SWI for the detection of cerebral microhemorrhage in patients with TBI. *Neurol. Med. Chir*, 97-99.
23. Moen, K.G., Vik, A., Olsen, A., Skandsen, T., Haberg, A.K., Evensen, K.A. and Eikenes, L. (2016). Traumatic axonal injury: Relationships between lesions in the early phase and diffusion tensor imaging parameters in the chronic phase of traumatic brain injury. *J Neurosci Res* 94, 623-635.
24. Toth, A., Kornyei, B., Kovacs, N., Rostas, T., Buki, A., Doczi, T., Bogner, P. and Schwarcz, A. (2018). Both hemorrhagic and non-hemorrhagic traumatic MRI lesions are associated with the microstructural damage of the normal appearing white matter. *Behav Brain Res* 340, 106-116.



25. Conde, V., Andreasen, S.H., Petersen, T.H., Larsen, K.B., Madsen, K., Andersen, K.W., Akopian, I., Madsen, K.H., Hansen, C.P., Poulsen, I., Kammersgaard, L.P. and Siebner, H.R. (2017). Alterations in the brain's connectome during recovery from severe traumatic brain injury: protocol for a longitudinal prospective study. *BMJ open* 7, e016286.
26. Maas, A.I., Hukkelhoven, C.W., Marshall, L.F. and Steyerberg, E.W. (2005). Prediction of outcome in traumatic brain injury with computed tomographic characteristics: a comparison between the computed tomographic classification and combinations of computed tomographic predictors. *Neurosurgery* 57, 1173-1182; discussion 1173-1182.
27. Maas, A.I., Stocchetti, N. and Bullock, R. (2008). Moderate and severe traumatic brain injury in adults. *The Lancet. Neurology* 7, 728-741.
28. Brown, A.W. (2005). Clinical Elements that Predict Outcome after Traumatic Brain Injury: A Prospective Multicenter Recursive Partitioning (Decision-Tree) Analysis. *Journal of neurotrauma* 22, 1040-1051.
29. Giacino, J.T., Kalmar, K. and Whyte, J. (2004). The JFK Coma Recovery Scale-Revised: Measurement characteristics and diagnostic utility. *Archives of Physical Medicine and Rehabilitation* 85, 2020-2029.
30. Schnakers, C., Vanhaudenhuyse, A., Giacino, J., Ventura, M., Boly, M., Majerus, S., Moonen, G. and Laureys, S. (2009). Diagnostic accuracy of the vegetative and minimally conscious state: clinical consensus versus standardized neurobehavioral assessment. *BMC Neurol* 9, 35.
31. Ashley, M., O'Shanick, G, Kreber, L. (2009). Early vs. Late Treatment of Traumatic Brain Injury.: Brain Injury Association of America.
32. group, E.r. (2015). The Efficacy of Acquired Brain Injury Rehabilitation: ERABI Research Group.
33. Kellner, E., Dhital, B., Kiselev, V.G. and Reiser, M. (2016). Gibbs-ringing artifact removal based on local subvoxel-shifts. *Magn Reson Med* 76, 1574-1581.

34. Andersson, J.L., Skare, S. and Ashburner, J. (2003). How to correct susceptibility distortions in spin-echo echo-planar images: application to diffusion tensor imaging. *Neuroimage* 20, 870-888.
35. Smith, S.M., Jenkinson, M., Woolrich, M.W., Beckmann, C.F., Behrens, T.E., Johansen-Berg, H., Bannister, P.R., De Luca, M., Drobnjak, I., Flitney, D.E., Niazy, R.K., Saunders, J., Vickers, J., Zhang, Y., De Stefano, N., Brady, J.M. and Matthews, P.M. (2004). Advances in functional and structural MR image analysis and implementation as FSL. *Neuroimage* 23 Suppl 1, S208-219.
36. Adams, J.H. (1989). Diffuse axonal injury in head injury: definition, diagnosis and grading. *Histopathology* Volume 15, 49 - 59.
37. Whyte, J., Vasterling, J., Manley, G. T. (2010). Common data elements for research on traumatic brain injury and psychological health: current status and future development. *Arch Phys Med Rehabil* 91, 1692-1696.
38. Greenberg, S.M., Vernooij, M.W., Cordonnier, C., Viswanathan, A., Al-Shahi Salman, R., Warach, S., Launer, L.J., Van Buchem, M.A. and Breteler, M.M.B. (2009). Cerebral microbleeds: a guide to detection and interpretation. *The Lancet Neurology* 8, 165-174.
39. Tong, K., Holshouser, B., Wu, Z. (2011). Chapter 11. Traumatic Brain Injury. In: *Susceptibility Weighted Imaging in MRI: Basic Concepts and Clinical Applications*. Mark Haacke, J.R. (ed). Wiley-Blackwell.
40. Debette, S. and Markus, H.S. (2010). The clinical importance of white matter hyperintensities on brain magnetic resonance imaging: systematic review and meta-analysis. *BMJ (Clinical research ed.)* 341, c3666.
41. Wardlaw, J.M., Valdes Hernandez, M.C. and Munoz-Maniega, S. (2015). What are white matter hyperintensities made of? Relevance to vascular cognitive impairment. *J Am Heart Assoc* 4, 001140.

42. Carpentier, A., Galanaud, D., Puybasset, L., Muller, J.C., Lescot, T., Boch, A.L., Riedl, V., Cornu, P., Coriat, P., Dormont, D. and van Effenterre, R. (2006). Early morphologic and spectroscopic magnetic resonance in severe traumatic brain injuries can detect "invisible brain stem damage" and predict "vegetative states". *J Neurotrauma* 23, 674-685.
43. Smith, S.M., Johansen-Berg, H., Jenkinson, M., Rueckert, D., Nichols, T.E., Miller, K.L., Robson, M.D., Jones, D.K., Klein, J.C., Bartsch, A.J. and Behrens, T.E. (2007). Acquisition and voxelwise analysis of multi-subject diffusion data with tract-based spatial statistics. *Nature protocols* 2, 499-503.
44. Abu Hamdeh, S., Marklund, N., Lannsjö, M., Howells, T., Raininko, R., Wikström, J. and Enblad, P. (2017). Extended Anatomical Grading in Diffuse Axonal Injury Using MRI: Hemorrhagic Lesions in the Substantia Nigra and Mesencephalic Tegmentum Indicate Poor Long-Term Outcome. *J Neurotrauma* 34, 341-352.
45. Tong, K.A., Ashwal, S., Holshouser, B.A., Nickerson, J.P., Wall, C.J., Shutter, L.A., Osterdock, R.J., Haacke, E.M. and Kido, D. (2004). Diffuse axonal injury in children: clinical correlation with hemorrhagic lesions. *Ann Neurol* 56, 36-50.
46. Yasushi Shibata, A.M., Kotoo Meguro, Kiyoshi Narushima (2000). Differentiation of mechanism and prognosis of traumatic brain stem lesions detected by magnetic resonance imaging in the acute stage. *Clinical Neurology and Neurosurgery* 102, 124-128.
47. Nielsen, J.S., Dyrby, T.B. and Lundell, H. (2018). Magnetic resonance temporal diffusion tensor spectroscopy of disordered anisotropic tissue. *Scientific reports* 8, 2930.
48. Nilsson, M., Englund, E., Szczepankiewicz, F., van Westen, D. and Sundgren, P.C. (2018). Imaging brain tumour microstructure. *Neuroimage* 182, 232-250.
49. Wellman, G.C. and Koide, M. (2013). Impact of subarachnoid hemorrhage on parenchymal arteriolar function. *Acta Neurochir Suppl* 115, 173-177.
50. Ivanidze, J., Kallas, O.N., Gupta, A., Weidman, E., Baradaran, H., Mir, D., Giambone, A., Segal, A.Z., Claassen, J. and Sanelli, P.C. (2016). Application of Blood-Brain Barrier Permeability Imaging in Global Cerebral Edema. *AJNR Am J Neuroradiol* 37, 1599-1603.

51. Gennarelli, T.A., JH et al (1982). Diffuse axonal injury and traumatic coma in primates. *Annals of Neurology* 12, 564-574.
52. Zasler, N.K., DI. Zafonde, RD. (2007). *Brain Injury Medicine: Principles and Practice*. Demos Medical Publishing: New York.
53. Ommaya, A.K. (1995). Head injury mechanisms and the concept of preventive management: a review and critical synthesis. *J Neurotrauma* 12, 527-546.
54. Moe, H.K., Moen, K.G., Skandsen, T., Kvistad, K.A., Laureys, S., Haberg, A. and Vik, A. (2018). The Influence of Traumatic Axonal Injury in Thalamus and Brainstem on Level of Consciousness at Scene or Admission: A Clinical Magnetic Resonance Imaging Study. *J Neurotrauma*, 975-084.
55. Fuller, P.M., Sherman, D., Pedersen, N.P., Saper, C.B. and Lu, J. (2011). Reassessment of the structural basis of the ascending arousal system. *The Journal of comparative neurology* 519, 933-956.
56. Schiff, N.D. (2010). Recovery of consciousness after brain injury: a mesocircuit hypothesis. *Trends Neurosci* 33, 1-9.
57. Giacino, J.T., Fins, J.J., Laureys, S. and Schiff, N.D. (2014). Disorders of consciousness after acquired brain injury: the state of the science. *Nat Rev Neurol* 10, 99-114.

**Table 1: Patients' and healthy controls' characteristics**

VARIABLE	HEALTHY CONTROLS N=21	PATIENTS N=14
AGE (YEARS)	41 [18-68]	44 [18-77]
FEMALE/MALE	2/19	2/12
GCS AT INJURY [3-15]		3 [3-8]
ROTTERDAM SEVERITY SCORE		2 [1-4]
INJURY SEVERITY SCORE [1-75]		31 [16-59]
POST TRAUMATIC AMNESIA (DAYS)		207 [62-400]
TIME FROM INJURY TO SCAN (DAYS)		44 (26-81)
CRS-R SCORE AT THE TIME OF SCAN [0-23]		13 (1-23)

Age, post traumatic amnesia time (PTA) and time from injury till project MRI are reported as mean and range. Female to male subjects are reported as a ratio. The remaining scores are reported as median and range. GCS: Glasgow coma scale. CRS-R: coma recovery scale revised.

**Table 2: Number and volume of traumatic microbleeds**

Brain region	Traumatic microbleeds	
	NUMBER	VOLUME
	Median	(mm <sup>3</sup> )
	[range]	Mean (SD)
Fronto-temporal	56 [0-478]	3095 (3824)
Parieto-occipital	14 [0-181]	718 (1225)
Mid-sagittal	12 [0-72]	706 (996)
Brainstem	3 [0-44]	364 (487)
Basal ganglia-thalamus	14 [0-98]	535 (753)

SD: standard derivation.

## Legends to figures

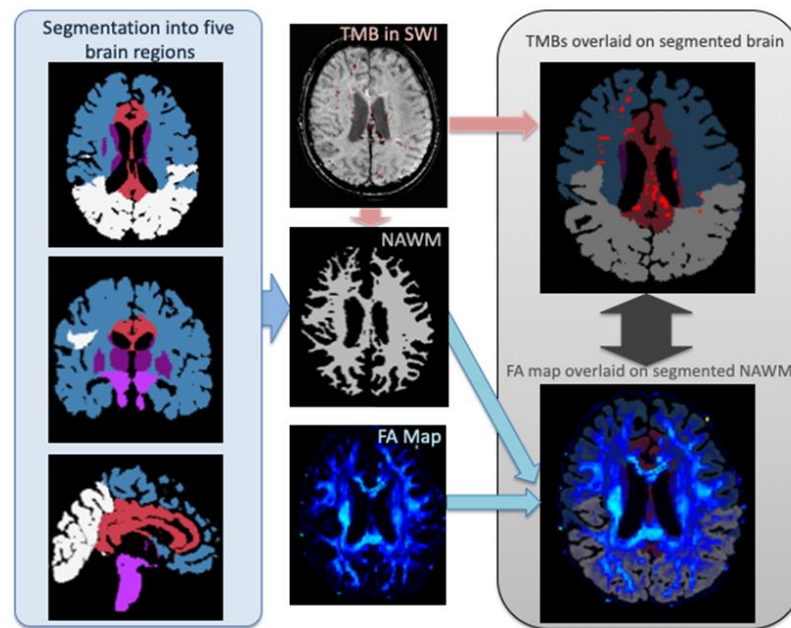


Figure 1

**Figure 1. Processing of MRI data**

T1-weighted brain images were segmented using Freesurfer software and the brain volumes were divided into five brain regions: fronto-temporal region (FT); parieto-occipital region (PO); corpus callosum and parasagittal WM (CC); brainstem (pons, midbrain and medulla) (BS); basal ganglia (caudate, putamen, pallidum) and thalamus (BT). White matter (WM) were also segmented using Freesurfer software and traumatic microbleeds and other lesions were excluded from the WM mask producing a normal appearing white matter (NAWM) mask. Fractional anisotropy (FA) and mean diffusivity (MD) were extracted from the NAWM in the five separate brain regions (MD is not represented in the figure, for a simplified overview).

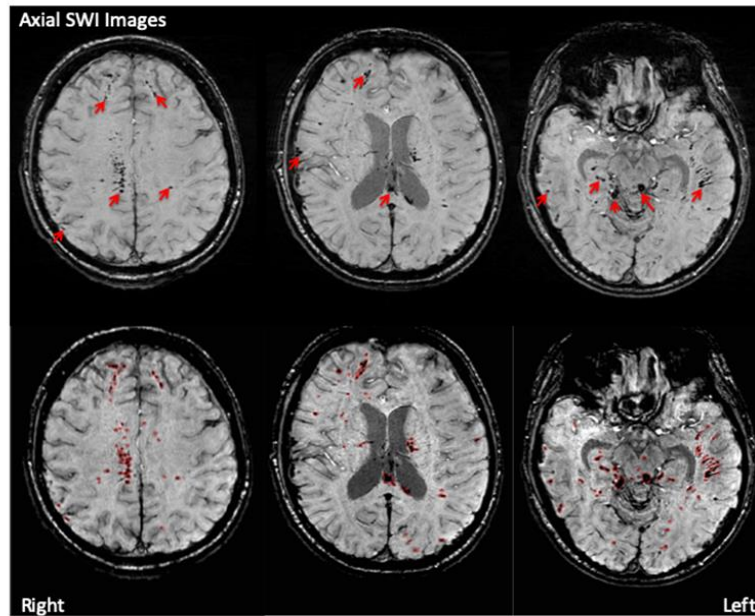
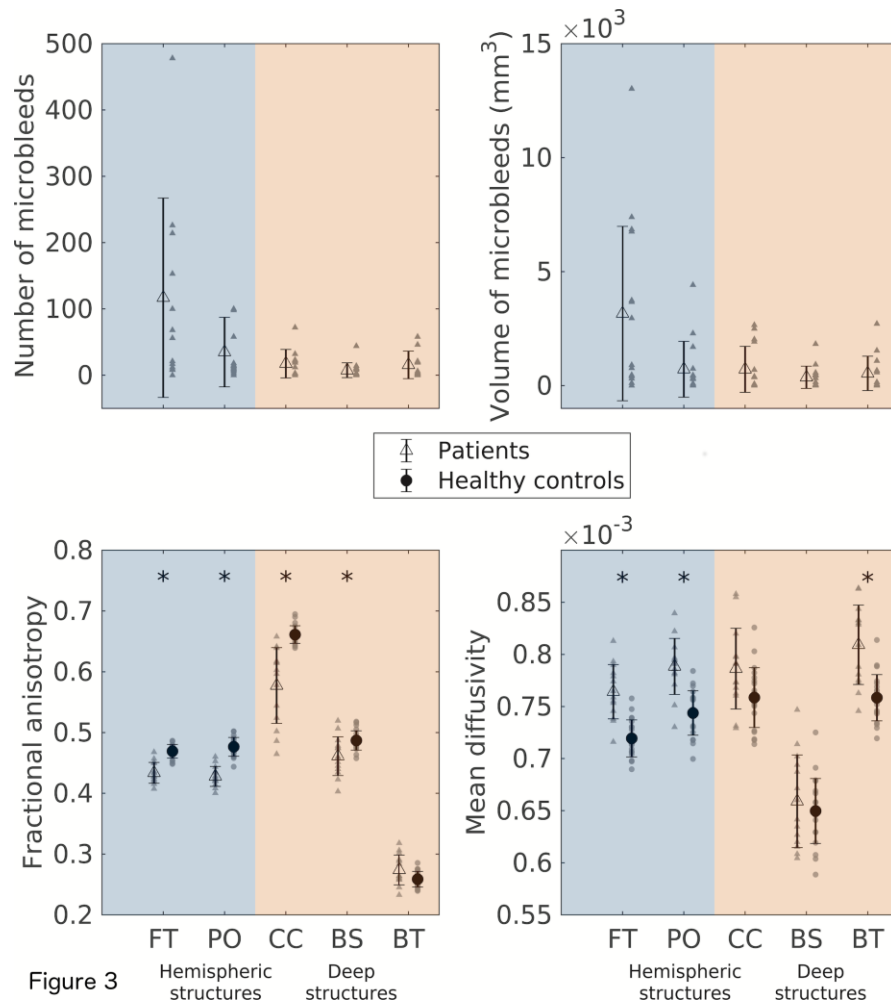


Figure 2

**Figure 2. Delineation of traumatic microbleeds in a single patient**

Axial brain slices showing hypointense lesions in susceptibility weighted imaging (SWI). These lesions (some of them highlighted by arrows) indicate traumatic microbleeds. The bottom panel shows the delineated traumatic microbleeds.





**Figure 3. Group data summarizing the microbleed distribution in patients (upper panels) and between- group differences in DTI-based microstructural metrics (lower panels).** Accumulated counts (top left) and volume (top right) of traumatic microbleeds in the five brain regions in patients with severe TBI. Bottom: Regional group differences in mean regional FA (left) and MD (right) between patients and healthy controls. The blue colour indicates regions belonging to superficial and lateral parts of the hemisphere. The light red color marks data derived from deep midline brain structures. The asterisk indicates  $p < 0.01$ . For all regions except for the basal ganglia-thalamus (gray matter), only voxels with  $FA > 0.3$  were used. FT: fronto-temporal region. PO: parieto-occipital region. CC: corpus callosum and parasagittal white matter. BS: brainstem (pons, midbrain and medulla). BT: basal ganglia (caudate, putamen, pallidum) and thalamus.

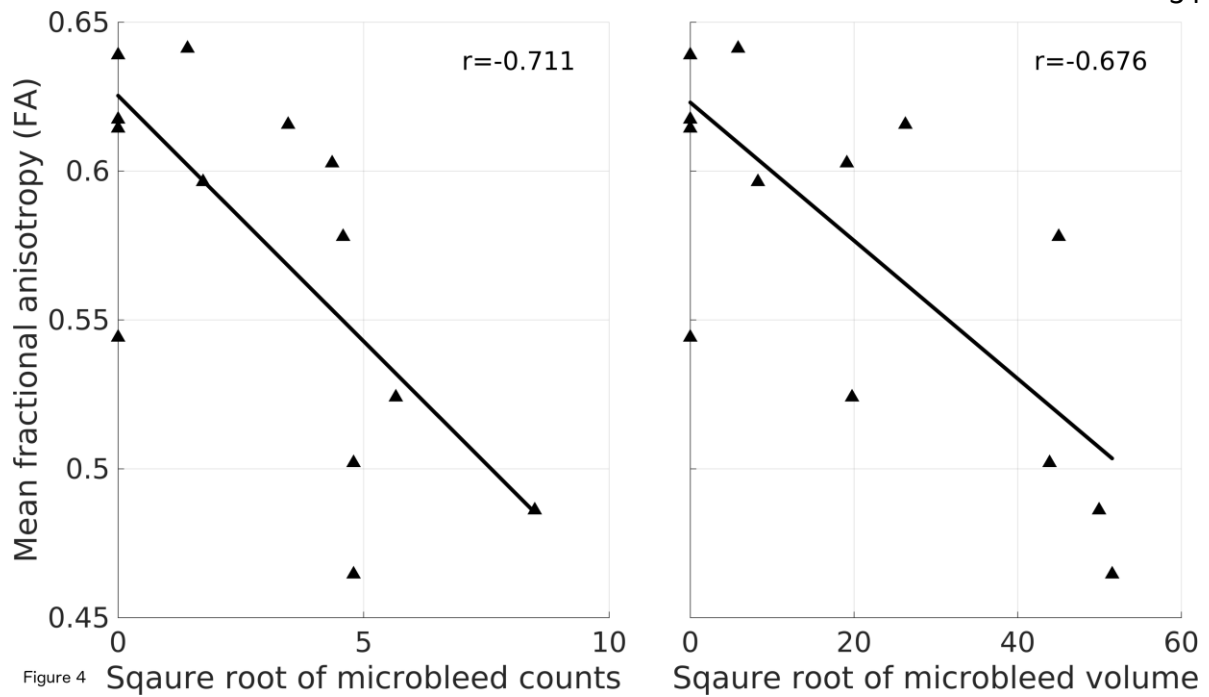


**Figure 4. Relation between regional microbleed load and mean fractional anisotropy in the midsagittal brain region.** Scatter plots showing the negative linear relationship between the regional load of TMBs and regional FA in the midsagittal ROI indicated by the regression line and the related r-values ( $p < 0.05$ ). Each triangle represents the value of an individual patient.

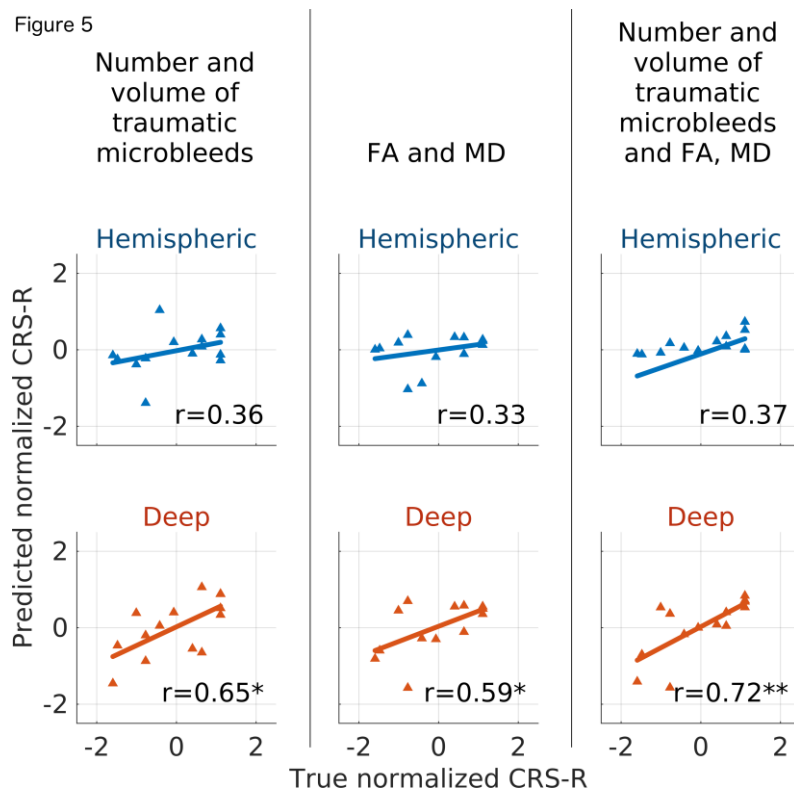


**Figure 5. Positive relationship between the predicted and the true observed Coma Recovery Scale Revised (CRS-R) score using hemispheric and deep brain structures.**

The top row is the hemispheric structures composed of the fronto-temporal and parieto-occipital regions. The bottom row is the deep brain structures composed of the midsagittal region (corpus callosum, cingulate and parasagittal white matter), the brainstem (pons, midbrain and medulla) and the basal ganglia (caudate, putamen, pallidum) and thalamus. The asterisk indicates  $p < 0.05$ ; The double asterisk indicates  $p < 0.01$ . Lines indicate best linear least-squares fit.

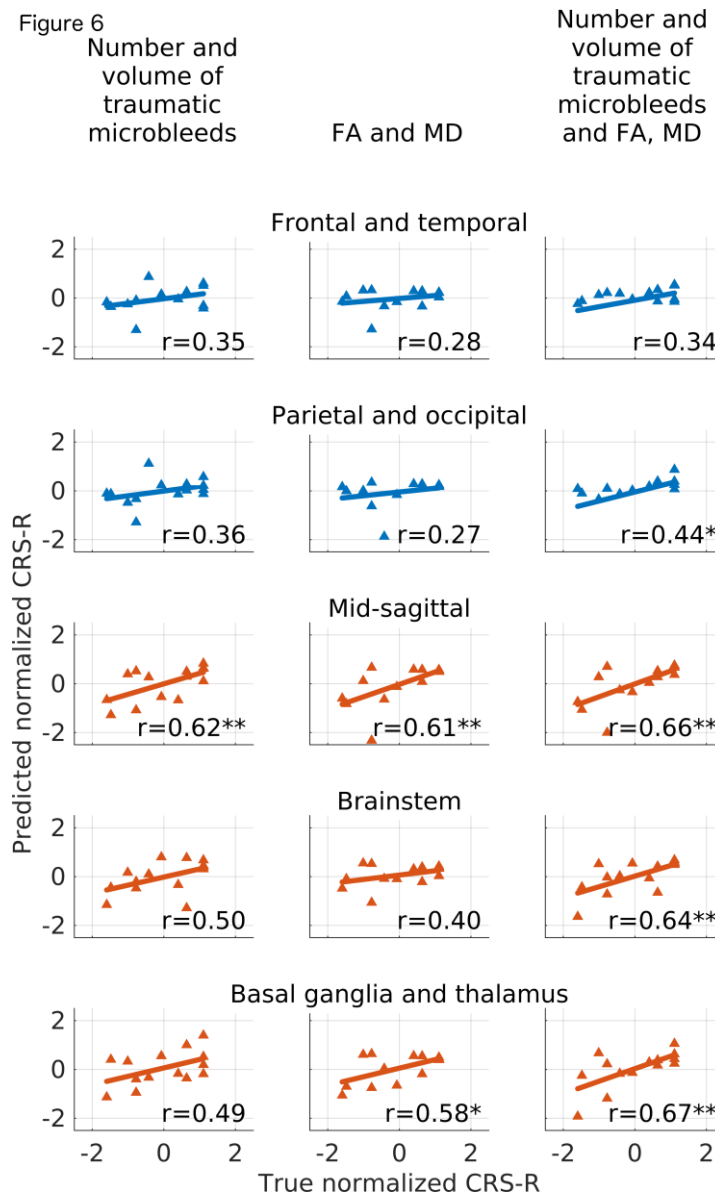


**Figure 6. Positive relationship between the predicted and the true observed Coma Recovery Scale Revised score using the individual five ROIs**

The color code of the plots refers to regional division into hemispheric (blue) and deep structures (light red). The asterisk indicates  $p < 0.05$ ; The double asterisk indicates  $p < 0.01$ . Lines indicate best linear least-squares fit.